ISSN 1070-3632, Russian Journal of General Chemistry, 2007, Vol. 77, No. 7, pp. 1148–1154. © Pleiades Publishing, Ltd., 2007.
Original Russian Text © E.A. Il'inchik, T.M. Polyanskaya, K.G. Myakishev, 2007, published in Zhurnal Obshchei Khimii, 2007, Vol. 77, No. 7, pp. 1064–1071.

Synthesis and Structure of the Complex $[Mo_3(\mu_3\text{-}S)(\mu_2\text{-}S_2)_3(Et_2NCS_2)_3]I$

E. A. Il'inchik, T. M. Polyanskaya, and K. G. Myakishev

Nikolaev Institute of Inorganic Chemistry, Siberian Branch, Russian Academy of Sciences, pr. Akad. Lavrent'eva 3, Novosibirsk, 630090 Russia

Received October 20, 2006

Abstract — The structure of tri-μ_2-disulfido-μ_3-thiotris(diethyldithiocarbamato)-*S,S'-triangle*-trimolybdenum iodide $[Mo_3(\mu_3\text{-}S)(\mu_2\text{-}S_2)_3(Et_2NCS_2)_3]I$ was determined. The compound was characterized by differential thermal analysis and IR, Raman, and X-ray electronic spectroscopy.
DOI: 10.1134/S107036320707002X

Tri-μ_2-disulfido-μ_3-thiotris(diethyldithiocarbamato)-*S,S'-triangle*-trimolybdenum iodide $[Mo_3(\mu_3\text{-}S)\cdot(\mu_2\text{-}S_2)_3(Et_2NCS_2)_3]I$ {$[Mo_3S_7dtc_3]I$}, where dtc = Et_2NCS_2), belongs to derivatives of the cluster ion $[Mo_3S_7]^{4+}$, which are fairly resistant to strong acids and oxidizing agents [1–3]. The enhanced interest to complexes of the series $[Mo_3S_7dtc_3]X$ (X = Cl^-, Br^-, etc.) is caused by the ability of axial sulfur atoms (S_a) of the cation disulfide groups μ_2S_2 to form short c ontacts with an X^- anion, $r(S_a–X)$, whose nature depends on the type of the anion [1–7]. As follows from extended Huckel theory (EHT) calculations [1], the formation of these contacts is associated with the covalent component of the $S_a\cdots X$ bond. In particular, the calculated atomic charges in the model compound $[Mo_3S_7(HCS_2)_3]Cl$ are as follows: q(Cl) –0.373, q(Mo) 0.213, $q(S_e)$ –0.025, and $q(S_a)$ 0.031. The available published evidence shows that the stretching vibration frequency of the disulfide groups ν(S–S) correlates with the lengths of the sulfur–sulfur bonds in the disulfide groups $r(S_a–S_e)$ and sulfur–X bonds $r(S_a–X)$ [1–7].

The compound $[Mo_3S_7dtc_3]I$ completes the short series of $[Mo_3S_7dtc_3]X$ compounds (X is halogen). Fedin et al. [2] and we failed to synthesize $[Mo_3S_7dtc_3]F$ because of the high reactivity of fluorine. At present five works dedicated to the synthesis and study of the $[Mo_3S_7dtc_3]I$ structure are known [1–3, 5, 6]. Crystallographic characteristics of the synthesized compounds are given in Table 1. X-ray structural data were obtained in [3, 6] for compounds with the proposed composition $[Mo_3S_7dtc_3]I$. However, later it was found [1, 7] that $[Mo_3S_7dtc_3]I$ was never obtained pure. The composition of compounds containing the $[Mo_3S_7dtc_3]^+$ cation depends on synthesis conditions [1, 7]. When another halogen is present in the starting materials or solvent, as a rule, a mixture of the target compound and a compound containing the other halide anion is formed. When the mixture is crystallized, solid solutions are mainly formed, for example, $[Mo_3S_7dtc_3]Br_{0.113}I_{0.887}$ [1, 3] and $[Mo_3S_7dtc_3]Cl_{0.53}Br_{0.47}$ [7]. In all the above-mentioned works, compounds containing the second halogen were used in the synthesis, and, therefore, the purity of the products could no be guaranteed. Lu et al. [6] used CuCl in the synthesis. Therefore, the resulting compound most likely is a solid solution of $[Mo_3S_7dtc_3]Cl_xI_{1-x}$ based on the $[Mo_3S_7dtc_3]Cl$ structure, but not a pure $[Mo_3S_7dtc_3]I$ salt, which is evidenced by the overestimated thermal factor of the iodine atom [6] and too short C–C bond in the ethyl fragment, r(C–C) 1.26(2) Å (usual length of this bond is ~1.50 Å [8]).

As seen from Table 1, the crystallographic parameters of the $[Mo_3S_7dtc_3]I$ complex are rather sensitive to halogen and solvent admixtures.

In this work we obtained $[Mo_3S_7dtc_3]I$ according to Eq. (1) which is similar to that proposed in [2], i.e. under conditions excluding presence of another halide ion, and studied the structure and physicochemical properties of this compound.

$$2[Mo_3S_7dtc_3]dtc + CdI_2 = 2[Mo_3S_7dtc_3]I + Cd(dtc)_2. \quad (1)$$

The crystal structure of $[Mo_3S_7dtc_3]I$ synthesized in this work differs from those reported in [1–3, 5–6]. It contains two crystallographically independent cluster cations $[Mo_3S_7dtc_3]^+$ and two crystallographically independent anions I^- (Fig. 1). The geometry

Table 1. Crystallographic characteristics of compounds containing the $[Mo_3S_7dtc_3]I$ ion pair

Composition	Symmetry	Space group	*a*, Å	*b*, Å	*c*, Å	β, deg	*Z*	Reference
$[Mo_3S_7dtc_3]I \cdot 0.5CH_2Cl_2$	rhombic	*Aba*2	24.782(2)	17.849(3)	16.429(3)		8	[1, 3]
$[Mo_3S_7(dtc)_3]I_{0.887}Br_{0.113}$	rhombic	*Iba*2	17.761(3)	24.281(4)	16.74(1)		8	[1, 3]
$[Mo_3S_7(dtc)_3]I \cdot 1.5C_6H_6$	rhombohedral	$R\bar{3}c$	13.707(1)		76.654(1)		12	[2]
$[Mo_3S_7(dtc)_3]I \cdot S_8 \cdot 2CH_2Cl_2$	monoclinic	$P2_1/n$	11.881(2)	15.559(4)	26.197(7)	98.53(2)	4	[5]
$[Mo_3S_7(dtc)_3]I$	monoclinic	$P2_1/n$	14.396(3)	13.116(3)	18.142(8)	91.36(3)	4	[6]
$[Mo_3S_7(dtc)_3]I$	rhombic	$Pna2_1$	24.593(3)	16.989(2)	16.983(4)		8	This work

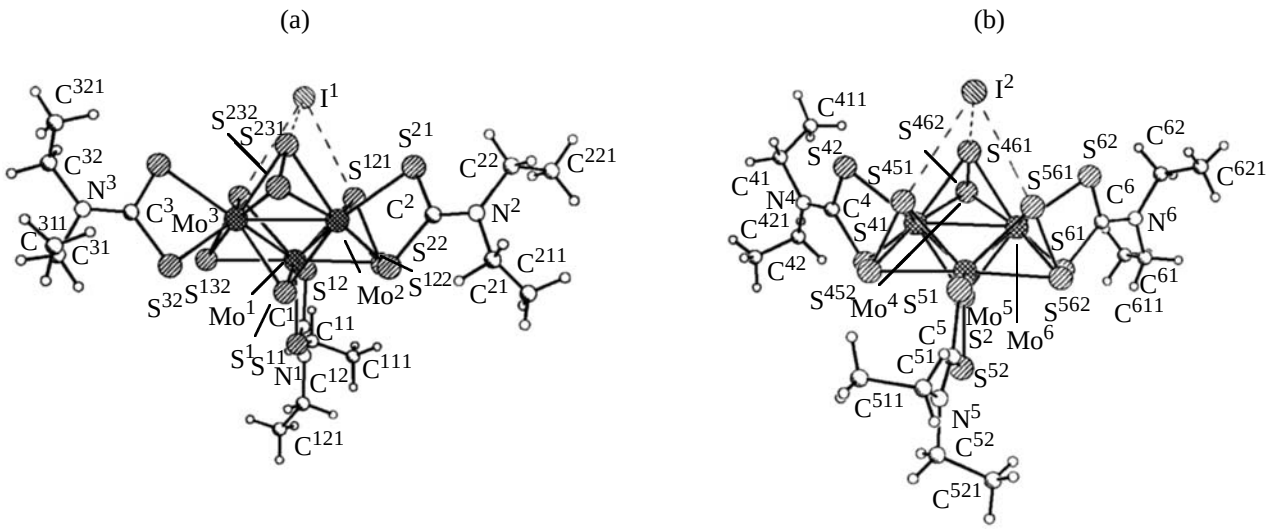

Fig. 1. Structure of $[Mo_3S_7dtc_3]I$ (short cation–anion contacts are shown by dashed lines). (a) Groups of equivalent sulfur atoms in cation 1: equatorial (S_e): S^{121}, S^{131}, and S^{231}; axial (S_a): S^{122}, S^{132}, and S^{232}; sulfur atoms of the dtc^- ligands in the *trans* position to μ_3-S (S_{trans}): S^{11}, S^{21}, and S^{31} and in the *cis* position (S_{cis}): S^{12}, S^{22}, and S^{32}; and (μ_3-S): S^1. (b) Groups of equivalent sulfur atoms in cation 2: (S_e): S^{451}, S^{461}, and S^{561}; (S_a): S^{452}, S^{462}, and S^{562}; S_{trans}): S^{41}, S^{51}, and S^{61}; (S_{cis}): S^{42}, S^{52}, and S^{62}; and (μ_3-S): S^2.

of the $Mo_3S_7^{4+}$ cluster fragments is similar to that described in the literature [1-7]. In the clusters, the three Mo atoms form an equilateral triangle with the average Mo–Mo bond length of 2.717(1) Å. The average length of the Mo_3–S bond is 2.365(2) Å. The ligands S_2 are coordinated in the η^2 mode. Each pair of Mo atoms coordinates the bridging μ_2S_2 ligand so that the three equatorial atoms S_e reside almost in the Mo_3 plane, whereas the three axial S_a atoms reside on the side opposite to the μ_3S atom. The fact that the S_a atoms come out of the plane of the Mo_3 triangle allows them to be arranged closer to Mo atoms by ~0.060 Å compared to the S_e atoms. The average S_a–S_e distance in the μ_2S_2 ligands is 2.048(3) Å. Three dtc^- ligands coordinate Mo atoms in a bidentate mode to form almost planar four-membered rings perpendicular to the Mo_3 plane. The sulfur atoms involved in the chelate rings locate unsymmetrically relative to the Mo_3 plane. The average MoMoS angle for the sulfur atoms *trans* to μ_3S is larger by 17.9° compared to the respective angle for the sulfur atoms in the *cis* position and comprises 143.3°. The bond lengths in the MoS_2CNEt_2 fragments have usual values, according to the Cambridge structural databank [8].

A special feature of $[Mo_3S_7dtc_3]I$, as well as previously studied cation–anion salts with chloride, bromide, and iodide anions, is short anion–cation contacts resulting in the formation of ion pairs. The average length of axial $3S_a \cdots I^-$ contacts is 3.288(3) Å. This is much shorter less than the sum of the van der Waals radii of sulfur and iodine (3.95 Å [9]). The value found in this work is slightly larger than those found in the solid solution $[Mo_3S_7dtc_3]Br_{0.113}I_{0.887}$ (3.249 Å [1, 3]) and in solvated iodides of the same cluster cation with guest molecules {$[Mo_3S_7dtc_3]I \cdot 0.5CH_2Cl_2$ 3.269 Å [1], $[Mo_3S_7dtc_3]I \cdot 1.5C_6H_6$ 3.252 Å [2], and $[Mo_3S_7dtc_3]I \cdot S_8 \cdot 2CH_2Cl_2$ 3.257 Å

[5]}. Similar contacts in the above-mentioned monoclinic modification of $[Mo_3S_7dtc_3]I$ [6] are even shorter (3.205 Å on the average). This fact provide further evidence for our proposal that Lu et al. [6] dealt with a solid solution. In fact, in parallel with the decrease of the van der Waals radius in the series I → Br → Cl, the $3S_a\cdots I^-$ contacts in $[Mo_3S_7dtc_3]I$ should be longer than in solid solutions $[Mo_3S_7dtc_3]X_yI_{1-y}$, where X = Cl or Br. The average length of axial $3S_a\cdots Br^-$ contacts in $[Mo_3S_7dtc_3]Br$ is 3.105(2) Å [4] vs. 3.055 Å in $[Mo_3S_7dtc_3]Cl_{0.53}Br_{0.47}$ [7] and 2.997 Å in $[Mo_3S_7dtc_3]Cl$ [10]. The presence of solvated solvent molecules, too, results in shortening of the $3S_a\cdots I^-$ contacts.

The supramolecular structure is primarily formed by contacts involving $2\mu_3S$, $3S_e$, and $2S_{cis}$ atoms (Fig. 2a), rather than axial contacts. The structure is characterized by zigzag chains parallel to the *a* axis (the longest period) of the unit cell, and cations in the chains alternate as B–A–B–A–B–A. The translational unit contains four 2A+2B clusters. The μ_3S atoms of each cation, two S_e atoms of the A cluster, one S_e atom of the B cluster, and the S_{cis} atoms of the A and B clusters take part in supramolecular interactions. In this case, the μ_3S and S_{cis} atoms of each cation contact with the same S_e atom of the next cation. The observed contacts are sharply differentiated: Contacts involving S_{cis} atoms are the shortest [3.283 (a) and 3.337 Å (b)], whereas contacts involving μ_3S atoms are the longest [3.482 (c) and 3.437 Å (d)]. The S_e atom of the B cation form an additional short contact of 3.350 Å (e) with the S_e atom of the A cation, that takes no part in contacts with μ_3S and S_{cis}. As a result, each A cation is bound by two contacts with the neighbor B at the left side and by three contacts with the neighbor B to the right of it, and each B cation, on the contrary, is bound by three contacts with the neighbor A at the left side and by two, with the neighbor A at the right side. Iodine atoms frame the chains from the outside.

Note that similar compounds with Cl^- and Br^- anions have a 2D supramolecular layer structure containing 6^3 graphite nets whose nodes are occupied by Mo_3S_{13} clusters (Fig. 2b). The iodine compound synthesized in [6] belongs to the same structural type. This fact gives further evidence showing that this compound is a solid solution with two halide anions, viz. chloride and iodide.

The IR spectrum of $[Mo_3S_7dtc_3]I$ by and large coincides with the spectrum of $[Mo_3S_7dtc_3]Br$ [4]. An exception is provided by the ν(S–S) band of the disulfide μ_2S_2 groups, whose maximum in the spectrum of $[Mo_3S_7dtc_3]I$ is shifted to the low-frequency region to 520 cm^{-1}. The Raman spectra of $[Mo_3S_7dtc_3]I$ and $[Mo_3S_7dtc_3]Cl$ are shown in Fig. 3. These spectra, too, have noticeable differences in the region of libration vibrations and stretching vibrations of disulfide groups: In $[Mo_3S_7dtc_3]I$ the ν(S–S) band has maxima at 522 and 516 cm^{-1}, whereas in $[Mo_3S_7dtc_3]Cl$, at 544, 536, and 529 cm^{-1}. The maxima of the respective band in the $[Mo_3S_7dtc_3]Br$ complex are at 539 and 532 cm^{-1} [4]. The observed decrease in the ν(S–S) frequency is, according to [1], caused by the elongation of the S–S bond in the disulfide groups in going from $[Mo_3S_7dtc_3]Br$ (*r* 2.040) [4] and $[Mo_3S_7dtc_3]Cl$ (*r* 2.041) [10] to $[Mo_3S_7dtc_3]I$ (*r* 2.048 Å).

Atomic charges in compounds can be judged about by the bond energies of their inner electrons (*E*). In a rough approximation, *δ* is proportional to effective atomic charge. The results of an X-ray photoelectron study (XPE) of the $[Mo_3S_7dtc_3]X$ series (Table 2) show that variation of X^- scarcely affects the electron density distribution in the $[Mo_3S_7dtc_3]^+$ cation. The *E*(X) values found for ammonium halides [12, 13], binuclear $Pt_2(CH_3CONH)_4X_2$ complexes (with an essentially ionic nature of the Pt–X bond) [14], and $[Mo_3S_7dtc_3]X$ are close to each other. This fact suggests that the effective charges of the X^- anions in the $[Mo_3S_7dtc_3]X$ complexes and ammonium salts are roughly equal to each other and close to –1 [12]. Therefore, the formation of short $3S_a\cdots X$ contacts in the $[Mo_3S_7dtc_3]X$ salts is not connected with an appreciable electron density transfer from the anion to cation.

The charge on Mo atoms, corresponding to the Pauling charge q_p(Mo), can be obtained from the empirical chemical shift–charge correlation (2) [15].

$$2[Mo3d_{5/2}] = 3.33q_p + 228.0. \quad (2)$$

This charge is positive and equal to 0.5 e. The average Pauling charge on sulfur atoms q_p(S) can be determined from the correlation dependence presented graphically in [16]. Algebraically, this dependence takes form (3).

$$E(S2p) = 5.2q_p + 163.8. \quad (3)$$

The resulting q_p(S) value of –0.1 is averaged over S atoms in the $[Mo_3S_7dtc_3]$ cation [11, 17]. As the $[Mo_3S_7dtc_3]^+$ cation contains 13 sulfur atoms, their total charge is –1.3. Therefore, the charge of the cluster nucleus consisting of 3 molybdenum and 13 sulfur atoms is +0.2. It is obvious that the missing part of the cation charge is localized in the dtc^- ligands. The resulting pattern of the electron density

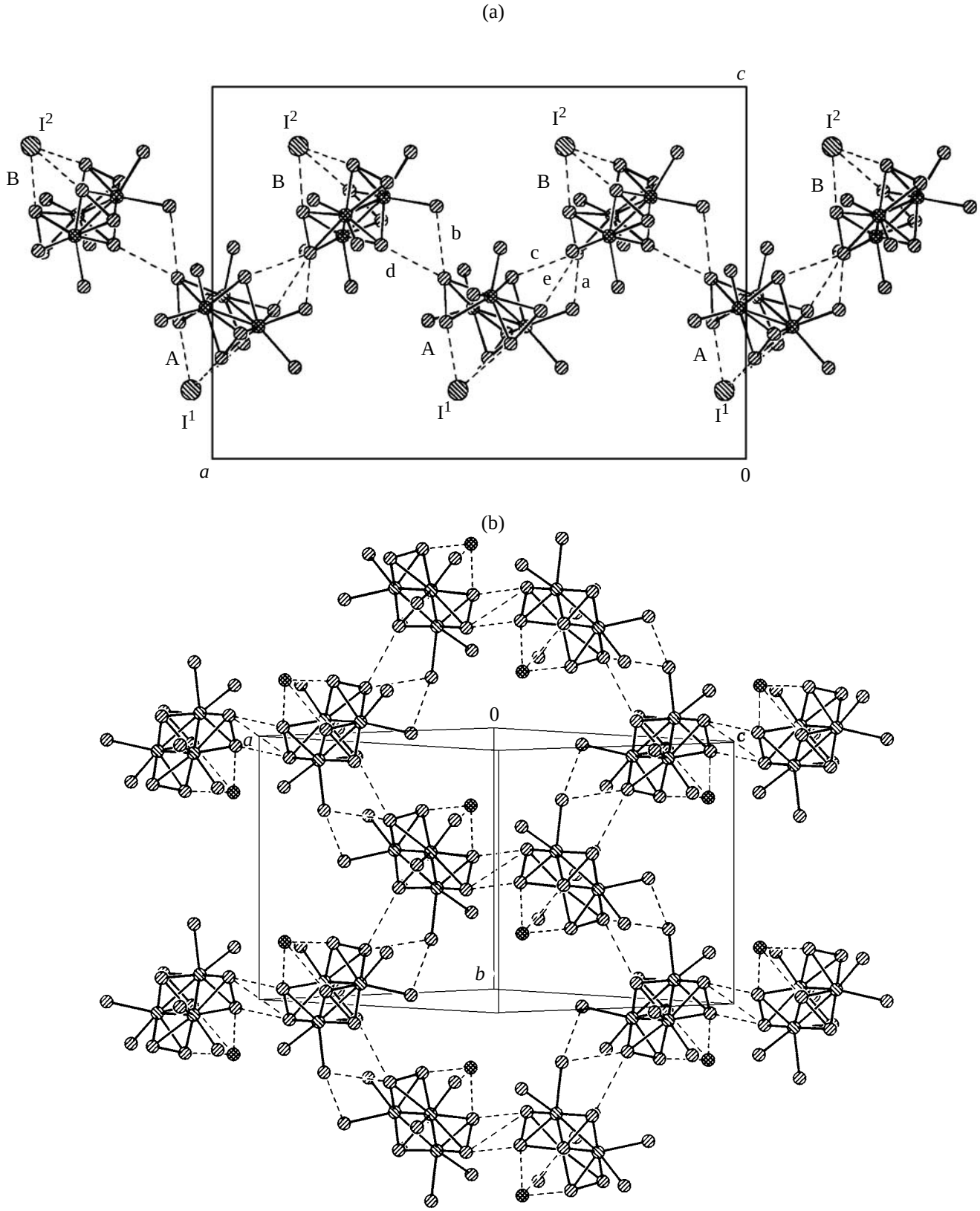

Fig. 2. Fragments of supramolecular structures. (a) 1D structure of $[Mo_3S_7dtc_3]I$, projected on the (010) plane, (b) 2D structure of $[Mo_3S_7dtc_3]X$ (X = Cl, Br). Shown are only nuclei of Mo_3S_{13} clusters, short X···S and S···S contacts are shown by dashed lines.

Table 2. Bond energies of inner electrons *E*, eV

Compound	Mo3$d_{5/3,3/2}$	Mo3$p_{3/2}$	N1*s*	S2*p*	S2*s*	Halogen[a]	Reference
$[Mo_3S_7dtc_3]dtc$	229.7(1.4)[b] 232.9(1.3)	395.6(2.3)	400.2(1.7)	163.0(2.5) 161.7 sh	227.4 226.1 sh		[11]
$[Mo_3S_7dtc_3]Cl$	229.7(1.7) 232.9(1.5)	395.6(2.6)	400.3(1.8)	163.3(2.7)	227.5	197.2(2.5)	This work
$[Mo_3S_7dtc_3]Br$	229.6(1.6) 232.8(1.5)	395.5(2.6)	400.3(1.7)	163.3(2.7)	227.5	68.0(2.5)	[4]
$[Mo_3S_7dtc_3]I$	229.7(1.8) 232.9(1.6)	395.5(2.7)	400.3(1.8)	163.3(2.8)	227.5	618.5(2.2)	This work
Bu_4NCl						197.3(3.3)	[12]
RMe_3NBr[c]						67.7	[13]
$Pt_2(CH_3CONH)_4Cl_2$						198.2	[14]
$Pt_2(CH_3CONH)_4Br_2$						68.9	[14]
$Pt_2(CH_3CONH)_4I_2$						619.3	[14]

[a] Cl2$p_{3/2}$, Br3$d_{5/2}$, and I3$d_{5/2}$. [b] Parenthesized in the half-width of the spectral contour $\Delta_{1/2}$, eV. [c] R = $C_{16}H_{33}$; *E*(Br3$d_{5/2}$) was reduced to the standard *E*(C1*s*) value of 285.0 eV accepted in this work.

distribution in the cation qualitatively agrees with the EHT calculation for the model compound $[Mo_3S_7 \cdot (HCS_2)_3]Cl$ [1]: *q*(Mo) 0.21, *q*(S) –0.03 (averaged over 13 atoms), and *q*(Mo_3S_{13}) +0.24. The calculation points to a considerable covalent contribution in the $S_a \cdots Cl$ bonds, which contradicts the above-presented evidence in favor of an essentially ionic nature of $[Mo_3S_7dtc_3]X$ salts. This is also supported by the effective charges on the Cl atom in $[Mo_3S_7dtc_3]Cl$, estimated from the chemical shift–charge correlation dependence (4) based on ab initio calculations [18].

$$E(\text{Cl}2p) = 4.25q(\text{Cl}) + 201.2. \quad (4)$$

The charge on the C1 atom is –0.94.

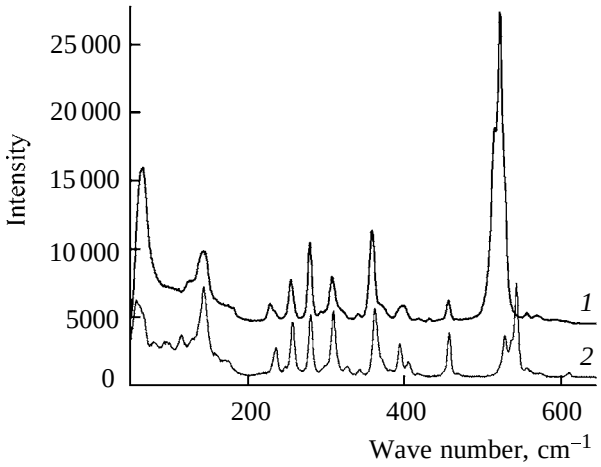

Fig. 3. Raman spectra of (*1*) $[Mo_3S_7dtc_3]I$ and (*2*) $[Mo_3S_7dtc_3]Cl$.

The resolution of our method is insufficient to differentiate the electron density distribution between different nonequivalent groups of sulfur atoms in the cation. Nevertheless, we can note that the $\Delta_{1/2}$ values for the Mo3$d_{5/2}$ and S2*p* lines of $[Mo_3S_7dtc_3]dtc$ are higher than those for MoS_2 by only 0.1 and 0.3 eV, respectively [15]. This finding points to equivalence of Mo atoms in the cation, on the one hand, and to a more or less uniform electron density distribution over different nonequivalent groups of S atoms, on the other. The experimental spectrum of the S2$p_{3/2,1/2}$ electrons of $[Mo_3S_7dtc_3]Cl$ and the theoretical spectrum forme using the S atomic charges in the model compound $[Mo_3S_7(HCS_2)_3]Cl$ [1], calculated by the EHT method, are shown in Fig. 4. The S2$p_{3/2}$ and S2$p_{1/2}$ spectral components corresponding to separate groups of equivalent sulfur atoms were approximated using the Lorentz distribution with a half-width of 1.5 eV. The spin–orbit splitting is 1.0 eV [20]. The position of the maximum on the energy scale was determined by Eq. (3) on the assumption that EHT charges correspond to Pauling charges. The theoretical spectrum (curve 2) is displaced by 0.4 eV to higher bond energies and has a well-defined high-energy shoulder. The half-width of the contour is 2.3 eV, which is smaller by 0.5 eV than that of the experimental contour (curve *1*). By varying positions of separate S2$p_{3/2,1/2}$ components on the energy scale we can construct a model spectrum (Fig. 5, curve *6*) whose shape and parameters [*E*(S2*p*) 163.3 and $\Delta_{1/2}$ 2.8 eV] are consistent with experiment (Table 2). The maxima of components *1*–*5* of this contour are at 162.6, 163.0, 163.3, 163.8, and 162.9 eV, respectively. From this it follows that the effective charge of the

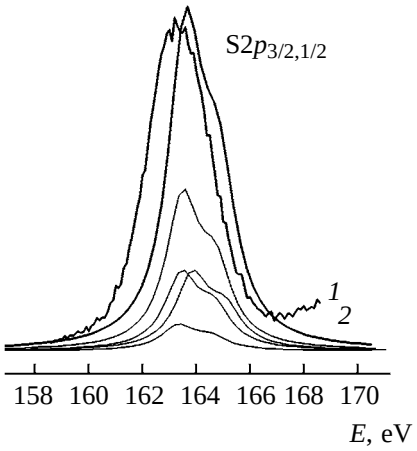

Fig. 4. (*1*) Experimental and (*2*) theoretical S2$p_{3/2,1/2}$ spectra of the $[Mo_3S_7dtc_3]Cl$ complex.

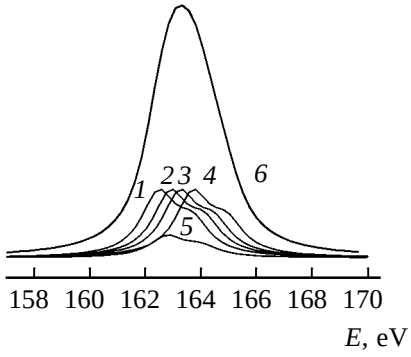

Fig. 5. (*6*) Simulated S2$p_{3/2,1/2}$ spectrum of the $[Mo_3S_7dtc_3]Cl$ complex. The absence of fine structure is provided by an almost equidistant arrangement of spin doublets *1*–*5*, each belonging to one group of equivalent S atoms.

sulfur atoms of the dtc ligands and μ_2S_2 disulfide groups vary over a fairly wide range (from 0 to –0.23 on the Pauling scale). Evidence for the uniform charge distribution is provided by the fact that in the $[Mo_3S_7dtc_3]Cl$ complex the Mo–S bond lengths in these ligands vary over a fairly wide range for each group of equivalent S atoms: $r(MoS_a)$ 2.401–2.418, $r(Mo–S_e)$ 2.467–2.495, $r(Mo–S_{trans})$ 2.455–2.480, and $r(Mo–S_{cis})$ 2.517–2.534 Å [10]. Taking into account lability of S_a atoms and the results of the EHT calculation [1], the effective charge close to zero [E(S2p) 163.8 eV] may well be assigned to this group atoms. In this respect, the XPE data confirm the results of the EHT calculation [1]. However, the above experimental data show that the calculation strongly overestimates the covalent contribution to the short contacts of axial sulfur atoms with the anion.

EXPERIMENTAL

The single crystal X-ray diffraction analysis of $[Mo_3S_7dtc_3]I$ was performed on an Enraf–Nonius CAD-4 automatic four-circle diffractometer. The unit cell parameters and the intensities of 6064 reflexes, 5925 of which are unique, were measured at 20(1)°C on a $0.44 \times 0.16 \times 0.12$ mm crystal ($\lambda Mo K_\alpha$ radiation, graphite monochromator, ω scanning, $\theta \le 25°$). Three control reflexes were measured every 97 reflexes; no essential variations were observed. Crystals of $[Mo_3S_7dtc_3]I$, $C_{15}H_{30}IMo_3N_3S_{13}$, reddish-brown, rhombic, at 20°C: a 24.593(3), b 16.989(2), c 16.983(4) Å, V 7096(2) Å^3, Z 8, d_{calc} 2.029 g cm^{-3}, μ 2.694 mm^{-1}, space group $Pna2_1$.

The intensities were corrected for Lorentz factors and polarization, absorption corrections were derived from two azimuthal scan curves. The structure was identified by the direct method [21] in combination with difference Fourier syntheses and refined by full-matrix least squares in the anisotropic approximation for non-hydrogen atoms, using the SHELX 97 program [22]. Hydrogen atoms were localized geometrically and refined in the rigid body approximation. The final divergence factors $R(F)$ 0.0243 and $wR(F^2)$ 0.0385 were determined for 4564 unique reflexes with $F > 4\sigma_F$, $R(F)$ 0.0355 for all 5925 unique reflexes.

The IR spectra were recorded on a UR-20 spectrophotometer in KBr and Nujol. The Raman spectra of solid samples were recorded on a Triplemate Spex spectrometer equipped with a microscope at the input and a multichannel detector at the output, excitation with a He–Ne laser (λ 632.3 nm) in the back scattering geometry.

The bond energies of inner electrons were measured on a VG ESCALAB spectrometer, AlK_α excitation. The spectrometer was calibrated by the Au4$f_{7/2}$ (84.0 eV), Ag3$d_{5/2}$ (368.2 eV), and Cu2$p_{3/2}$ (932.6 eV) lines. The external standard was the C1s line (285.0 eV) of hydrocarbons present as contamins on sample surface. A finely ground substance was rubbed into a double-sided adhesive tape (scotch). The bond energies were determined with an accuracy of ±0.1 eV.

The device for DTA experiments was described in [23], reference Al_2O_3, Chromel–Alumel thermocouple, heating rate 6 deg min^{-1}, initial resolution 1.3 Pa, sample 0.1 g.

Complex $[Mo_3S_7dtc_3]I$. Acetonitrile, 10 ml, was added to a mixture of 0.1 g of $[Mo_3S_7dtc_3]dtc$ and 0.045 g of CdI_2 (molar ratio 2:3, which corresponds to a double excess of CdI_2), and the mixture was re-

fluxed for 30 min. The product was filtered off, washed with acetonitrile, and dried in air to obtain 0.105 g of a fine orange-yellow powder containing a small amount of colorless rod-like crystals whose composition and properties were not investigated. The target compound was prepared by recrystallization from DMF. The IR spectrum of the compound is identical to the spectrum of $[Mo_3S_7dtc_3]Br$ [4], but the maximum of the ν(S–S) band is observed at 520 cm^{-1} (Nujol). Raman spectrum (Fig. 3, spectrum *1*), ν, cm^{-1}: 522 vs, 516 s, 456 w, 431 vw, 397 ww, 358 s/m, 341 vw, 307 m, 294 vw, 279 s/m, 255 m, 228 w, 142 m, 126 w, 66 s. Found, %: Mo 26.6; S 38.2; I 11.9. $C_{15}H_{30}IMo_3N_3S_{13}$. Calculated, %: Mo 26.5; S 38.4; I 11.7.

According to DTA in combination with gas volumetry, $[Mo_3S_7dtc_3]I$ decomposes without melting in three stages. The weak endo effect at 314°C corresponds to the initiation of gas evolution. The second and third strong endo effects are observed at 334 and 380°C, respectively. Gas evolution stops practically simultaneously with the completion of the third endo effect at ~400°C. The volume of the evolved gas was ~85 l mol^{-1} starting compound, weight loss 43%. The decomposition pattern of $[Mo_3S_7dtc_3]I$ differs only slightly from those of $[Mo_3S_7dtc_3]Cl$ and $[Mo_3S_7 \cdot dtc_3]Br$ [4].

Complex $[Mo_3S_7dtc_3]Cl$ was obtained by the procedure given in [10]. Its Raman spectrum is shown in Fig. 3 (spectrum *2*).

ACKNOWLEDGMENT

The authors are grateful to A.V. Virovets for help in the X-ray diffraction study, A.I. Boronin for recording the XPS spectra, and B.A. Kolesov for recording the Raman spectra.

REFERENCES

1. Mayor-Lopez, M.J., Weber, J., Hegetschweiler, K., Meienberger, M.D., Joho, F., Leoni, S., Nesper, R., Reiss, G.J., Frank, W., Kolesov, B.A., Fedin, V.P., and Fedorov, V.E., *Inorg. Chem.*, 1998, vol. 37, no. 11, p. 2633.
2. Fedin, V.P., Muller, A., Bege, Kh., Armatazh, A., Sokolov, M.H., Yarovoi, S.S., and Fedorov, V.E., *Zh. Neorg. Khim.*, 1993, vol. 38, no. 10, p. 1677.
3. Zimmermann, H., Hegetschweiler, K., Keller, T., Gramlich, V., Schmalle, H.W., Petter, W., and Schneider, W., *Inorg. Chem.*, 1991 vol. 30, no. 23, p. 4336.
4. Il'inchik, E.A., Polyanskaya, T.M., Myakishev, K.G., Basova, T.V., and Kolesov, B.A., *Zh. Obshch. Khim.*, 2002, vol. 72, no. 12, p. 1968.
5. Wang, M.-F., Quo, G.-C., Huang, J.-S., Zhuang, H.-H., Zhang, Q.-E., and Lu, J.-X., *Chin. J. Struct. Chem. (Jiegou Huaxue)*, 1994, vol. 13, no. 3, p. 221.
6. Lu, C.-Z., Tong, W., Zhuang, H.-H., and Wu, D.-M., *Chin. J. Struct. Chem. (Jiegou Huaxue)*, 1993, vol. 12, no. 2, p. 124.
7. Virovets, A.V. and Volkov, O.V., *Zh. Strukt. Khim.*, 2000, vol. 40, no. 4, p. 866.
8. Allen, F.H. and Kennard, O., *Chem. Design Automat. News*, 1993, vol. 8, no. 1, p. 31.
9. Batsanov, S.S., *Zh. Neorg. Khim.*, 1991, vol. 36, no. 12, p. 3015.
10. Fedin, V.P., Sokolov, M.N., Geras'ko, O.A., Virovets, A.V., Podberezskaya, N.V., Fedorov, V.Ye., *Inorg. Chim. Acta*, 1992, vol. 192, no. 2, p. 153.
11. Myakishev, K.G., Polyanskaya, T.M., and Il'inchik, E.A., *Zh. Obshch. Khim.*, 2000, vol. 70, no. 10, p. 1585.
12. Folkesson, B. and Larsson, R., *Chem. Scripta*, 1976, vol. 10, no. 3, p. 105.
13. Wagner, C.D., *J. Vac. Sci. Technol.*, 1978, vol. 15, no. 2, p. 518.
14. Salyn', Ya.V., Nefedov, V.I., Maiorova, A.G., and Kuznetsova, G.N., *Zh. Neorg. Khim.*, 1978, vol. 23, no. 3, p. 829.
15. Grim, S.O. and Matienzo, L.J., *Inorg. Chem.*, 1975, vol. 14, no. 5, p. 1014.
16. Lindberg, B.J., Hamrin, K., Johansson, G., Fahlman, A., Nordling, C., and Siegbahn, K., *Phys. Scripta*, 1970, vol. 1, no. 3, p. 286.
17. Il'inchik, E.A., Volkov, V.V., Volkov, O.V., Asanov, I.P., and Kolesov, B.A., *Koord. Khim.*, 2000, vol. 26, no. 3, p. 192.
18. Sundberg, P., Larsson, R., and Folkesson, B., *J. Electron Spectrosc.*, 1988, vol. 46, no. 1, p. 19.
19. Patterson, T.A., Carver, J.C., Leyden, D.E., and Hercules, D.M., *J. Phys. Chem.*, 1976, vol. 80, no. 15, p. 1700.
20. Best, S.A., Brant, P., Feltham, R.D., Rauchfuss, Th.B., Roundhill, D.M., and Walton, R.A., *Inorg. Chem.*, 1977, vol. 16, no. 8, p. 1976.
21. Altomare, A., Cascarano, G., Giacovazzo, C., Guagliardi, A., Moliteruc, A.G.G., Burla, M.C., Polidori, G., Camalli, M., and Spagna, R., Abstracts of Papers, *17th Eur. Crystallogr. Meeting*, Lissboa, 1997, p. 65.
22. Sheldrick, G.M., *SHELX-97*, Release 97-2, Göttingen: Univ. of Göttingen, 1997.
23. Volkov, V.V. and Myakishev, K.G., *Izv. Sib. Otd. Akad. Nauk SSSR, Ser. Khim.*, 1977, vol. 5, no. 12, p. 111.